

Correcting correlated errors for quantum gates in multi-qubit systems using smooth pulse control

Xiu-Hao Deng,^{1,2,*} Yong-Ju Hai,¹ Jun-Ning Li,³ and Yao Song¹

¹*Shenzhen Institute of Quantum Science and Engineering,
Southern University of Science and Technology, Shenzhen, Guangdong 518055, China*

²*Guangdong Provincial Key Laboratory of Quantum Science and Engineering
Southern University of Science and Technology, Shenzhen, Guangdong 518055, China*

³*Department of Physics, City University of Hong Kong,
Tat Chee Avenue, Kowloon, Hong Kong SAR, China*

In multi-qubit system, correlated errors subject to unwanted interactions with other qubits is one of the major obstacles for scaling up quantum computers to be applicable. We present two approaches to correct such noise and demonstrate with high fidelity and robustness. We use spectator and intruder to discriminate the environment interacting with target qubit in different parameter regime. Our proposed approaches combines analytical theory and numerical optimization, and are general to obtain smooth control pulses for various qubit systems. Both theory and numerical simulations demonstrate to correct these errors efficiently. Gate fidelities are generally above 0.9999 over a large range of parameter variation for a set of single-qubit gates and two-qubit entangling gates. Comparison with well-known control waveform demonstrates the great advantage of our solutions.

Quantum error correction provides a path to large-scale universal quantum computers. But it is built on challenging assumptions about the characteristics of the underlying errors in quantum logic operations to be statistically independent and uncorrelated [1–3]. In realistic environments error sources could exhibit strong temporal or spatial correlations [4], cannot be corrected efficiently using close-loop quantum error correction. In a multi-qubit system, due to massive control lines and compact geometric structure, a qubit is unavoidably to interact with other quantum systems including qubits, couplers, neighbor control lines [5], etc. This introduces control crosstalk [6], leakage [7], parameter shift, decoherence and gate errors when operating on target qubit(s). Noises become spatially-correlated, making qubits more fragile and gate calibrations more complicated. The simultaneous gate error rate dramatically increases compared to isolated case as qubit system grows [2, 7–9]. To better isolate the qubits and suppress the unwanted interactions, the state-of-art techniques rely on tunable qubits and tunable couplers [7, 10–14]. The costs of introducing the tunability are that more control lines and more crowded spectral. Tuning over large regions of qubits’ or couplers’ frequency crosses more anti-crossing points, where adiabatic dynamics causes additional errors [7, 11–14]. These obstacles limit the applications of current qubit systems and slow down the development of scalable quantum computers.

In the NISQ era, open-loop quantum error correction (QEC) technique is essentially important [15]. As an example of QEC techniques, dynamical decoupling (DD) are successfully applied to further isolate target qubits from the environment [16–18], hence also corrects the correlated errors due to unwanted couplings. But it is difficult to apply DD sequences during a quantum gate oper-

ation to increase the fidelity [19]. Further, dynamically-corrected gate (DCG) are proposed to suppress small dephasing errors [18, 20, 21]. Traditional DCG relies on sequences of operation which takes the multiple times of gate depth increases as the expense for a better single gate. Similar to DD, use of simple pulses, such as square or δ -function, could easily cause serious waveform distortion [22], which brings in additional operation errors and limits the realistic application of DD and DCG. Smooth pulse DCG has been proposed to implement single qubit gates [18, 23, 24] to enhance the robustness of quantum gates subject to local static noise. How to correct the errors induced during entangling two qubits is unexplored. Also, a most drawback of conventional DCG models is the assumption of small errors. When errors becomes significant and non-perturbative, DCG fails.

In this paper, we study how to dynamically suppress or correct the errors in multi-qubit system, especially the errors induced by unwanted interactions. We analyze these errors in two different coupling regime with reference to the control strength. For different regime, we propose different approaches to targeted correct the errors in the relevant regime. Our approaches are combinations of analytical theory and numerical methods, which could give unlimited solutions of smooth control pulses for universal gate sets. We present some examples of our solutions which are demonstrated numerically with high fidelities. Our approach could be applied to implement robust gates but also single qubit gate for qubit with always-on interaction with other qubits, as well as to resolve other issues in current stage of multi-qubit quantum computers. Our approaches provides a set of dynamical corrected gates for qubit even with always-on interaction. In such case, tunable couplers are not necessarily needed for scalable quantum processors any more.

Errors in Multi-qubit system.—Qubits couple to each other in a multi-qubit system, target qubit spectrum is observed to be either splitted or broadened depending on the coupling strength, as Fig.1(b) shows. Its Hamiltonian in eigenbasis of a two-level subspace takes the form

$$H_t^{diag} = -\frac{\delta}{2}\sigma_z \quad (1)$$

in rotating frame with ω_t , where t stands for "target" and δ corresponds to level-splitting or parameter fluctuation. δ is generally nonvanishing in various qubit systems, including two-level system (TLS) and multi-level system (MLS) such as superconducting transmon qubits, as well as in various interaction regime. Analytical forms of δ in different regime are derived in supplementary [25].

Large interaction between qubits gives benefit to entangling operations but harms single qubit operations. As what is used to be done in quantum dots and superconducting qubits, detuning target qubit from the interacted qubits could reduce the effective coupling strength but can't decouple them [26, 27]. While effective coupling gets much stronger than decoherence rate, target qubit's Stark splittings [28] are visible and its transition frequency in isolated-basis $|0\rangle_t \longleftrightarrow |1\rangle_t$ splits for δ in the dressed basis (eigenbasis), corresponding to subspace $\text{span}\{|0\rangle_i|0\rangle_t, |0\rangle_i|1\rangle_t\}$ and $\text{span}\{|1\rangle_i|0\rangle_t, |1\rangle_i|1\rangle_t\}$. And we call this scenario the *intruded regime* and the coupled quantum systems are intruders, with subscript "i". Gate operations in this regime suffer from control-rotation correlated errors. This issue is especially serious for fix frequency qubits. The bipartite Hamiltonian is diagonalized as $H_t^{diag} = \text{diag}\{\{-\frac{\omega}{2}, \frac{\omega}{2}\}, \{-\frac{\omega+\delta}{2}, \frac{\omega+\delta}{2}\}\}$ as shown in supplement. The second subspace could be transformed back to Eq.1. Note that when the target is coupled to multiple quantum systems, its spectrum split to multiplets, with the Hamiltonian in the n^{th} subspace of the target qubit as $H_{tn}^{diag} = (-\frac{\omega}{2} + \delta_n)\sigma_{z,t}$.

Current trending technique is to apply tunable couplers [7, 11–14] to connect qubits with the cost of more control lines and complexity of chip design. The tunability could be designed to realize very high on/off ratio, which lead to successful demonstration of quantum supremacy [7]. But with the realistic limit to the tunability and imperfection of geometrical isolation, residual coupling is still a problem for precise gate operations [7, 12, 29][citations]. Small couplings compared to decoherence makes level-splitting invisible but broadens absorption peak, meaning a measured enhancement of decoherence rate, see Fig.1(b). The inset shows the increased decoherence rate subject to the broadening of measured absorption. Also with the tunable coupler, parameter fluctuations in the coupler could introduces correlated noise to the two operated qubits during an entangling gate. We call this regime the *spectated regime*. The coupled quantum systems are called spectators.

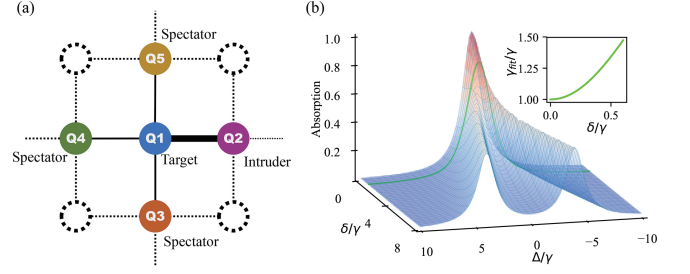


FIG. 1: (a) Schematic figure of multi-qubit system shows the target qubit interacting with spectators and intruders. The thicker of the link between qubits, the stronger residual coupling remains. (b) simulates the observed absorption versus Δ and effective ZZ-coupling δ , for non-correlated decoherence rate $\gamma = 1 \text{ MHz} \times 2\pi$. At $\delta_c \approx 0.7 \text{ MHz} \times 2\pi$ split peaks combine as a single peak. Hence it is the transition point between the spectated regime intruded regime. When coupling strength is small $\delta < \delta_c$, the doublet's absorption overlap with each other and combined as one broadened peak, resulting in enhanced dephasing rate. Green line is the fitting curve of the resultant absorption profile at $\delta = 0.5 \text{ MHz} \times 2\pi$. Numerical fitting of decoherence rate $\gamma^{fit} = 1.341 \text{ MHz} \times 2\pi$, using a combination line shape of Lorentzian and Gaussian. The inset shows the fitting decoherence rate enhancement versus δ .

Besides Stark effect, inhomogeneous driving strength and control crosstalk errors could be induced via unwanted couplings to intruders or spectators. The ladder operators, which the control field couples to, are modified in the dressed basis. Take an example of a bipartite system $H_0 = -\frac{\omega_i}{2}\sigma_z^i - \frac{\omega_t}{2}\sigma_z^t + g\sigma_x^i\sigma_x^t$ with the xy control in bare-basis $H_{st}^d = \Omega(t)(\sigma_t^+ e^{i\omega_d t} + h.c.)$, the coupling matrices in eigenbasis is

$$\tilde{\sigma}_t^+ = \begin{bmatrix} -\frac{\Delta+\epsilon}{\Upsilon_+} & \\ \frac{2g}{\Upsilon_+} & -\frac{\Delta+\epsilon}{\Upsilon_-} & \frac{2g}{\Upsilon_-} \end{bmatrix} \quad (2)$$

where $\epsilon = \sqrt{4g^2 + \Delta^2}$, $\Delta = \omega_i - \omega_t$, $\Upsilon_{\pm} = \sqrt{4g^2 + (\sqrt{4g^2 + \Delta^2} \pm \Delta)^2}$. $\Omega(t)$ drives transitions $|\widetilde{00}\rangle \leftrightarrow |\widetilde{01}\rangle$ and $|\widetilde{10}\rangle \leftrightarrow |\widetilde{11}\rangle$ with inhomogeneous dipole moments, as well as crosstalk on transitions $|\widetilde{00}\rangle \leftrightarrow |\widetilde{10}\rangle$ and $|\widetilde{01}\rangle \leftrightarrow |\widetilde{11}\rangle$.

As well known that in solid state qubit system, low frequency noise is one of the major intrinsic error sources [30–32]. Usually gate operations are much shorter than qubit's life time by several orders of magnitude, hence the low frequency nature of such noises behaves as a static error for quantum gates. The low frequency for a single qubit takes the same form as in Eq.1. While for a two-qubit operation such as $XX + YY$ interaction, the noise δ on target qubit 2 appears in the total Hamiltonian as this form

$$H^{total} = \begin{bmatrix} -\delta/2 & & & \\ & \delta/2 & g(t) & \\ & g(t) & -\delta/2 & \\ & & & \delta/2 \end{bmatrix} \quad (3)$$

The entangling dynamics is only affected in the two-level subspace $\text{span}\{|01\rangle, |10\rangle\}$ [33], hence the effective Hamiltonian again takes the same form as Eq.1 excluding the control field $\Omega(t) = g(t)$.

Targeted-correction gates in intruded regime.—In this regime, the level splitting δ is large, seen as splitted spectrum as Fig.1 (b). The Hamiltonian in the 4-by-4 computational subspace $\text{span}\{|\text{intruder}\rangle|\text{target}\rangle\}$ is diagonalized as $H^{diag} = \text{Diag}\{-\frac{\omega}{2}, \frac{\omega}{2}, -\frac{\omega+\Delta}{2}, \frac{\omega+\Delta}{2}\}$. Control-rotational error between the intruder and the target qubit is significant if using simple pulses, see the green dashed line in Fig.2 (b). Besides, a quantum gate targeted-correcting such errors needs to consider inhomogeneous dipole moments as shown in Eq.2. As pointed out above, implementing two-qubit entangling gates becomes relatively trivial in this regime compared to single qubit gates. A large ZZ interaction directly generates a CZ gate while large XX interaction implements an iSWAP gate. Here we present our targeted-correction gate (TCG) approach for given δ and dipole moment inhomogeneity to implement single qubit operations. First we decompose the $SU(4)$ dynamics to $SU(2) \otimes SU(2)$ dynamics. A control field $\tilde{H}_{st}^d = (\Omega^*(t)\tilde{\sigma}_t^+ e^{i\omega_d t} + h.c.)$ is added to the target qubit. Drive amplitude $\Omega(t)$ could be complex for IO control [citations] meaning driving both X and Y directions. Transformed to interaction picture with \tilde{H}_0 , the unitary operator

$$U^I(t) = \begin{bmatrix} U_1 & B \\ -B^\dagger & U_2 \end{bmatrix} \quad (4)$$

Because B includes fast oscillating phases $e^{i2\omega t}$ by taking $\omega_d = \omega$, it could be demonstrated that $B = 0$ under the constraints $\delta \ll \omega$ [25]. So the evolution operator is block diagonalized $U^{int}(t) = \text{Diag}\{U_1, U_2\}$. Since the first subspace $\text{span}\{|00\rangle, |01\rangle\}$ is driven resonantly $\omega_d = \omega$, $U_1(t) = \exp\{-i\frac{\Delta+\epsilon}{T_+} \int_{t_0}^{t_0+\tau_g} dt \Omega(t) \sigma_x\}$. For the second subspace $\text{span}\{|10\rangle, |11\rangle\}$, $U_2(t) = \mathcal{T} \exp\{-i\frac{2g}{T_-} \int_{t_0}^{t_0+T} dt [\Omega \cos(t\delta) \sigma_x - \Omega \sin(t\delta) \sigma_y]\}$. Generally, $U_1(t) \neq U_2(t)$, resulting in different trajectories depending on intruder's state, see Fig.2 (b) and (c). Setting $U_1(T) = U_{ideal}$ to get the area constraint $\frac{\Delta+\epsilon}{T_+} \int_{t_0}^T \Omega(t) dt = \theta_{ideal}/2$, where θ_{ideal} is the ideal rotational angle and T is the ending operation time. Setting $U_2(T) = U_1(T)$ to correct the control-rotational error, we get additional constraints $\frac{2g}{T_-} \int_{t_0}^T \Omega(t) \cos(\delta t) dt = \theta_{ideal}/2$ and $\int_{t_0}^T \Omega(t) \sin(\delta t) dt = 0$. We then apply

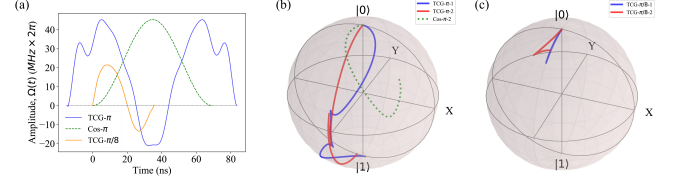


FIG. 2: (a) shows the waveform to implement π and $\pi/8$ gates at the present of an intruder, respectively in purple and orange. As an comparison, a widely used cosine waveform for X gate is shown as dashed line. (b) shows the trajectories of $|0_i 0_t\rangle \rightarrow |0_i 1_t\rangle$ and $|1_i 0_t\rangle \rightarrow |1_i 1_t\rangle$ operated by the TCG for a π X-rotation with fidelity 0.999, for comparison, added with a trajectory $|1_i 0_t\rangle \rightarrow |1_i 1_t\rangle$ operated by a widely used cosine pulse, which gives a fidelity 0.589. (c) shows the trajectories of $|0_i 0_t\rangle \rightarrow |0_i 1_t\rangle$ and $|1_i 0_t\rangle \rightarrow |1_i 1_t\rangle$ operated by the TCG for a $\pi/8$ X-rotation with fidelity 0.9999. These simulations use superconducting transmon qubits.

smooth pulse ansatz

$$\Omega(t) = \sum C_n \cos(2\pi \frac{nt}{T} + \phi_n) \quad (5)$$

to numerically search for appropriate waveforms for TCG of θ_{ideal} rotations. Results are shown in Fig.2. On the Bloch spheres, The quantum trajectories $|0\rangle_t \rightarrow |1\rangle_t$ and $|0\rangle_t \rightarrow \cos \frac{\pi}{16} |0\rangle_t + \sin \frac{\pi}{16} |1\rangle_t$ in different subspaces $\text{span}\{|00\rangle, |01\rangle\}$ and $\text{span}\{|10\rangle, |11\rangle\}$ demonstrated the idea of targeted-correction of π and $\pi/8$ XY gates [1]. A further numerical optimization using GRAB method [34], a GRAPE [35] assisted analytical optimization approach, could obtain fidelity > 0.9999 . The TCG pulse to implement the X gate shown in Fig.2(a) with the analytical formula Eq.5. For π gate, $C_n \in \{19.6, 17.5, -22.5, -0.7, 1.9, 0.5, 2.9, -4.6, -2.5, -2.8\} \text{ MHz} \times 2\pi$, and $\phi_n \in \{0.941, 1.883, -0.3701, 0.628, 1.580, 8.774, 0.3506, 1.346, 2.128\}$, $T = 98.6 \text{ ns}$. The fidelity is 0.998. While for $\pi/8$ gate, $C_n \in \{4.8, -17.7, -0.6, -1.1, -0.5, -0.4, -0.3, -0.2, -0.1, -0.1\} \text{ MHz} \times 2\pi$, and $\phi_n \in \{1.481, 8.663, 0.2454, 0.1687, 0.1230, 0.1042, 0.0747, -0.0134, 0.2745\}$, $T = 35 \text{ ns}$. The fidelity is 0.999. While allowing more harmonic components, both optimized fidelities are demonstrated to be above 0.99999. The numerical simulations here are demonstrated on superconducting transmon qubits connected via a coupler $H = \sum_j (\omega_j a_j^\dagger a_j - \frac{\alpha_j}{2} a_j^\dagger a_j^\dagger a_j a_j) + g_{cj} (a_c^\dagger + a_c)(a_j + a_j^\dagger)$, all with three levels. The parameters are $\omega_{1,2,c} = \{5.7735, 5.4735, 6.99\} \text{ GHz} \times 2\pi$, $\alpha_{1,2} = 249 \text{ MHz} \times 2\pi$, $g_{c1,c2} = 151 \text{ MHz} \times 2\pi$. The first subspace $\text{span}\{|00\rangle, |01\rangle\}$ is driven resonantly.

Errors robust gates in the spectated regime.—When the errors are small compared to decoherence rate γ . δ is close to the background fluctuations, hence the δ spreads over a range of $[-\Delta, \Delta]$. Instead of correcting a targeted value of δ , now the quantum gates should be robust to

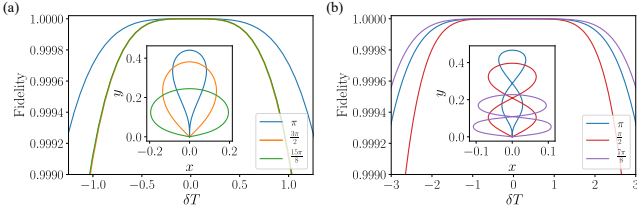


FIG. 3: Trajectories in parametrization space fidelities and of robust gates $\{\pi, \frac{\pi}{2}, \frac{\pi}{8}\}$ corresponding to colors blue, orange and green in (a) and (b). (a) shows the results of first order correction gates while (b) shows the results for correction gates up to second order errors. The high fidelity plateaus are generally above 0.99999 over a variation range of $\delta T = 1$ for 1st order cancellation and $\delta T = 2$ for 2nd order cancellation, with gate time 50 ns simulated for quantum dots.

this a range of errors. This requires a high fidelity plateau at $[-\Delta, \Delta]$ around $\delta = 0$. We take the perturbative approach of dynamically-corrected gate [18, 23, 24, 24] to find error-robust gates (ERG) in this regime [36]. Consider the noisy Hamiltonian with control fields

$$H = \begin{bmatrix} -\delta/2 & \Omega(t)e^{i\alpha(t)} \\ \Omega(t)e^{-i\alpha(t)} & \delta/2 \end{bmatrix} \quad (6)$$

The generated evolution operator $U = U_0 U_e$, where $U_0 = e^{-i \int_0^t H_0(\tau) d\tau}$ is the ideal evolution operator generated by $H_0 = \Omega \cos \theta \sigma_x - \Omega \sin \theta \sigma_y - \frac{\epsilon}{2} \sigma_z$. And $U_e = U_0^\dagger U = I - i \int_0^t H_e^I(\tau) d\tau + \int_0^t H_e^I(t_1) \int_0^{t_1} H_e^I(t_2) dt_2 dt_1 + O(\delta^2)$ is equivalent to the evolution in interaction picture, which could characterize the noisy evolution. The generator of U_e is $H_e^I = U_0^\dagger H_e U_0$, where $H_e = -\frac{\delta}{2} \sigma_z$. δ being small means $g \ll \Delta$ as derived in supplement, then $\frac{2g}{\Upsilon_+}, \frac{-\Delta + \sqrt{4g^2 + \Delta^2}}{\Upsilon_-} \rightarrow 0, \frac{\Delta + \sqrt{4g^2 + \Delta^2}}{\Upsilon_+}, \frac{2g}{\Upsilon_-} \rightarrow 1$, hence the dipole moments could be considered homogeneous. As a conclusion, correcting errors in this regime only concerns about the error δ in σ_z .

Since the operation $\frac{H_e^I(t)}{-\delta/2} = U_0^\dagger \sigma_z U_0$ is unitary with matrix norm $\left\| \frac{H_e^I(t)}{-\delta/2} \right\| = 1$, it could be mapped onto a point on a Bloch-like sphere [23]. The difference here is that this sphere represents the geometry of an operator instead of qubit states. So we parametrize $\frac{H_e^I(t)}{-\delta/2} = \vec{n}(t) \cdot \vec{\sigma}$, where $\vec{n}(t)$ is an analog of Bloch vector. The change of $\frac{H_e^I(t)}{-\delta/2}$ in terms of time could be characterized as a directional trajectory $\vec{r}(t_0 : t)$ on the parametrization sphere, starting from $\vec{r}(t_0)$ and ending at $\vec{r}(T)$ as finishing a gate. So $\left| \frac{H_e^I(t)}{-\delta/2} \right| = \left\| \frac{H_e^I(t)}{-\delta/2} \right\| = 1$, which defines time t in terms of the spherical parameters

$$t = \int_0^{\vec{r}} d\vec{r}'. \quad (7)$$

Also, since $\ddot{\vec{r}}(t) \cdot \vec{\sigma} = \frac{i}{\delta/2} U_0^\dagger [H_0, H_e] U_0$, the curvature of the curve $\vec{r}(t_0 : t)$ is proven [25] to define the control field

$$\Omega(t) = \ddot{\vec{r}}(t). \quad (8)$$

Further, the torque of \vec{r} [37]

$$\dot{\alpha}(t) = \frac{(\dot{\vec{r}} \times \ddot{\vec{r}}) \cdot \ddot{\vec{r}}}{\left\| \dot{\vec{r}} \times \ddot{\vec{r}} \right\|^2} \quad (9)$$

defines the rotational angle for the gate operation. Therefore, the overall evolution trajectory $U_0(t)$ generated by time-dependent Hamiltonian $H_0(t)$ could be fully determined in terms of Eq.7 to 9. Furthermore the pulse constraints for the ERG pulses could be determined. Since the gate fidelity subjects to errors $F(U_0 U_e, U_0) = \frac{1}{2} |Tr(U_e)|$, a ERG requires at $t = T$, $\frac{\partial(|Tr(U_e)|)}{\partial \delta} \rightarrow 0$. The first order correction gives $\partial \left(\frac{\delta}{2} Tr \left(\int_0^T dt \dot{\vec{r}}(t) \cdot \vec{\sigma} \right) \right) / \partial \delta = 0$. Similarly, the second

order correction requires $\int_0^T dt_1 \dot{\vec{r}}(t_1) \times \dot{\vec{r}}(t_1) = 0$, so on and so forth. Therefore, all the information about the parameter $\vec{r}(t)$ paves the way to look for any ERG pulses up to arbitrary order of correction. Our related work ref.[36] presents systematic construction of the ERG pulses.

As simple examples demonstrating the performance of ERG, we set $\alpha = 0$. Now $\vec{r}(t_0 : t)$ reduces to a directional curve on a two dimensional plane [18]. And the ideal rotational angle ϕ is reduced to this constraint

$$\phi = \arctan \left| \frac{\dot{\vec{r}}(T) \times \dot{\vec{r}}(0)}{\dot{\vec{r}}(T) \cdot \dot{\vec{r}}(0)} \right| = \Delta\varphi + \pi \text{ or } \Delta\varphi \quad (10)$$

We then find a universal gate set of ERG to implement single qubit X rotation with angles $\pi, \pi/2$ and $\pi/8$, see Fig.3. The fidelity is numerically calculated in a TLS with a range of fluctuation δ in σ_z . Wide range of high fidelity plateaus ($F > 0.99999$) are demonstrated both for first order and second order ERG. These plateaus are never obtained in commonly used pulses, such as Gaussian, Cosine, etc. Here, Cartesian coordinates $x = r \cos \theta, y = r \sin \theta$ are used to plot the parametrized curve, see the inset in Fig.3(a) and (b). Then we apply the π rotation curve to generate X gate as well as two qubit iSWAP gate for superconducting transmon qubits. Based on experimental parameters, the numerical results shown in Fig.4 also illustrate high fidelity plateaus for both single qubit operation and iSWAP. The ERG also exhibits certain robustness over pulse amplitude deviation (1 to 2% as shown in Fig.4(b) and (c)). The iSWAP fidelity plateau shifts to negative δ because

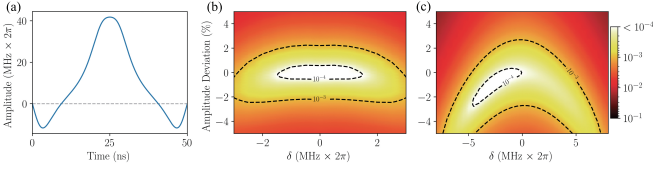


FIG. 4: Application of a first order π RG pulse, see (a), is applied to superconducting transmon qubit system to implement X gate and i SWAP gate, with the numerical simulation results shown in (b) and (c), respectively. The first order RG pulse is resolved from the π parametrized curve in Fig.3 (a). The parameters are $\omega_s = 5 \text{ GHz} \times 2\pi$, $\alpha_s = 230 \text{ MHz} \times 2\pi$, $\omega_t = 5.5 \text{ GHz} \times 2\pi$, $\alpha_t = 260 \text{ MHz} \times 2\pi$. The $XX + YY$ interaction strength g varies in the range $-58 < g < 58 \text{ MHz} \times 2\pi$ and $-100 < g < 100 \text{ MHz} \times 2\pi$ to obtains the range of δ in (b) and (c). Four levels are simulated for the transmons.

of the leakage to transmon's higher levels. Note that with the geometric formalism, finding appropriate pulses is still a challenging task and requires some techniques to systematical construction [36].

Discussion.—We have reported very promising approaches to correct spatial correlated errors in multi-qubit systems. We have firstly analyzed the mechanism of gate errors in multi-qubit system subject to spatial correlation. We have characterized two major regimes of couplings, and further studied in details the errors associated with spectators and intruders. To correct the errors induced by intruders, we propose targeted-correction gates to overcome not only level-splitting issue but also inhomogeneous control amplitudes. These two issues are by-passed by previous works. However, in some quantum computation or simulation tasks, operation qubit system in this regime provides lots of benefits. Now given our solutions, people could resolve these two issues potentially and go into a new paradigm of quantum computing with large always-on interactions. To correct the errors due to spectators, we propose error robust gates to produce high fidelity plateaus for a range of parameter variation. Compared to any conventionally-used pulses, our results lead great advantages on gate robustness for parameter variation. Also, the smoothness and limited-bandwidth of our pulses guarantee the waveform distortion under a controllable limit. For both scenarios, we have demonstrated exciting results with smooth and analytical pulses, high fidelities and powerful robustness. These results are supported with numerical simulations based on experimental parameters, which shows promising application in realistic multi-qubit quantum processors with current architecture or even allowing hardware simplifications.

Finally, we summarize some further observations of our approaches: 1. TCG provides an new paradigm for quantum computing or quantum simulation with always-on interaction, which is friendly for controlling fixed frequency qubits without increasing the complexity of control circuits; 2. Using ERG control, the residual cou-

pling issue on current architecture doesn't need to be eliminated; 3. TCG and ERG together opens up a new degree of control freedom; 4. Our approaches reduce the need for precise control of qubit frequency or tunable coupler. 5. Both TCG and ERG's results have small number of parameters for further optimization, which is very friendly for experiments.

This work was supported by the Key-Area Research and Development Program of Guangdong Province (Grant No. 2018B030326001), the National Natural Science Foundation of China (Grant No. U1801661), the Guangdong Provincial Key Laboratory (Grant No. 2019B121203002), the Guangdong Innovative and Entrepreneurial Research Team Program (Grant No. 2016ZT06D348), the Natural Science Foundation of Guangdong Province (Grant No. 2017B030308003), and the Science, Technology, and Innovation Commission of Shenzhen Municipality (Grants No. JCYJ20170412152620376 and No. KYT-DPT20181011104202253).

* Electronic address: dengxh@sustech.edu.cn

- [1] M. A. Nielsen and I. Chuang, "Quantum computation and quantum information," (2002).
- [2] J. Marques, B. Varbanov, M. Moreira, H. Ali, N. Muthusubramanian, C. Zachariadis, F. Battistel, M. Beekman, N. Haider, W. Vlothuizen, *et al.*, arXiv preprint arXiv:2102.13071 (2021).
- [3] Z. Chen, K. J. Satzinger, J. Atalaya, A. N. Korotkov, A. Dunsworth, D. Sank, C. Quintana, M. McEwen, R. Barends, P. V. Klimov, *et al.*, arXiv preprint arXiv:2102.06132 (2021).
- [4] J. Preskill, arXiv preprint arXiv:1207.6131 (2012).
- [5] E. S. Fried, P. Sivarajah, N. Didier, E. A. Sete, M. P. da Silva, B. R. Johnson, and C. A. Ryan, arXiv preprint arXiv:1908.11370 (2019).
- [6] P. Mundada, G. Zhang, T. Hazard, and A. Houck, *Physical Review Applied* **12**, 054023 (2019).
- [7] F. Arute, K. Arya, R. Babbush, D. Bacon, J. C. Bardin, R. Barends, R. Biswas, S. Boixo, F. G. Brandao, D. A. Buell, *et al.*, *Nature* **574**, 505 (2019).
- [8] M.-C. Chen, M. Gong, X. Xu, X. Yuan, J.-W. Wang, C. Wang, C. Ying, J. Lin, Y. Xu, Y. Wu, *et al.*, *Physical Review Letters* **125**, 180501 (2020).
- [9] M. Gong, M.-C. Chen, Y. Zheng, S. Wang, C. Zha, H. Deng, Z. Yan, H. Rong, Y. Wu, S. Li, *et al.*, *Physical review letters* **122**, 110501 (2019).
- [10] B. Foxen, C. Neill, A. Dunsworth, P. Roushan, B. Chiaro, A. Megrant, J. Kelly, Z. Chen, K. Satzinger, R. Barends, *et al.*, *Physical Review Letters* **125**, 120504 (2020).
- [11] T. Cai, X. Han, Y. Wu, Y. Ma, J. Wang, H. Zhang, H. Wang, Y. Song, and L. Duan, arXiv preprint arXiv:2101.01854 (2021).
- [12] J. Stehlik, D. Zajac, D. Underwood, T. Phung, J. Blair, S. Carnevale, D. Klaus, G. Keefe, A. Carniol, M. Kumph, *et al.*, arXiv preprint arXiv:2101.07746 (2021).
- [13] Y. Xu, J. Chu, J. Yuan, J. Qiu, Y. Zhou, L. Zhang, X. Tan, Y. Yu, S. Liu, J. Li, *et al.*, *Physical Review*

- Letters **125**, 240503 (2020).
- [14] M. C. Collodo, J. Herrmann, N. Lacroix, C. K. Andersen, A. Remm, S. Lazar, J.-C. Besse, T. Walter, A. Wallraff, and C. Eichler, *Physical Review Letters* **125**, 240502 (2020).
 - [15] J. Preskill, *Quantum* **2**, 79 (2018).
 - [16] J. Du, X. Rong, N. Zhao, Y. Wang, J. Yang, and R. Liu, *Nature* **461**, 1265 (2009).
 - [17] L. Viola, E. Knill, and S. Lloyd, *Physical Review Letters* **82**, 2417 (1999).
 - [18] J. Zeng, X.-H. Deng, A. Russo, and E. Barnes, *New Journal of Physics* **20**, 033011 (2018).
 - [19] X. Li, T. Cai, H. Yan, Z. Wang, X. Pan, Y. Ma, W. Cai, J. Han, Z. Hua, X. Han, *et al.*, *Physical Review Applied* **14**, 024070 (2020).
 - [20] K. Khodjasteh, D. A. Lidar, and L. Viola, *Physical review letters* **104**, 090501 (2010).
 - [21] K. Khodjasteh and L. Viola, *Physical review letters* **102**, 080501 (2009).
 - [22] S. Gustavsson, O. Zwiernik, J. Bylander, F. Yan, F. Yoshihara, Y. Nakamura, T. P. Orlando, and W. D. Oliver, *Physical review letters* **110**, 040502 (2013).
 - [23] E. Barnes, X. Wang, and S. D. Sarma, *Scientific reports* **5**, 1 (2015).
 - [24] J. Zeng, C. Yang, A. Dzurak, and E. Barnes, *Physical Review A* **99**, 052321 (2019).
 - [25] Supplementary.
 - [26] R. Hanson and D. D. Awschalom, *Nature* **453**, 1043 (2008).
 - [27] R. Barends, A. Shabani, L. Lamata, J. Kelly, A. Mezzacapo, U. Las Heras, R. Babbush, A. G. Fowler, B. Campbell, Y. Chen, *et al.*, *Nature* **534**, 222 (2016).
 - [28] N. B. Delone and V. P. Krainov, *Physics-Uspekhi* **42**, 669 (1999).
 - [29] R. A. Pinto, A. N. Korotkov, M. R. Geller, V. S. Shumeiko, and J. M. Martinis, *Physical Review B* **82**, 104522 (2010).
 - [30] F. Yoshihara, K. Harrabi, A. Niskanen, Y. Nakamura, and J. S. Tsai, *Physical review letters* **97**, 167001 (2006).
 - [31] R. C. Bialczak, R. McDermott, M. Ansmann, M. Hofheinz, N. Katz, E. Lucero, M. Neeley, A. O'connell, H. Wang, A. Cleland, *et al.*, *Physical review letters* **99**, 187006 (2007).
 - [32] E. Paladino, Y. Galperin, G. Falci, and B. Altshuler, *Reviews of Modern Physics* **86**, 361 (2014).
 - [33] J. Qiu and et al., "Dynamical decoupling of two-qubit interactions," (2021), (in preparation).
 - [34] Y. Song, Q.-h. Guo, J.-N. Li, and X.-H. Deng, "Smooth pulse optimization using grab assisted by auto-differentiation," (2021), (In preparation).
 - [35] N. Khaneja, T. Reiss, C. Kehlet, T. Schulte-Herbrüggen, and S. J. Glaser, *Journal of magnetic resonance* **172**, 296 (2005).
 - [36] Y.-J. Hai, Q.-h. Guo, Y. Song, and X.-H. Deng, "Constructing robust quantum gates using analytical functions," (2021), (in preparation).
 - [37] J. Lehto and K.-A. Suominen, *Journal of Physics A: Mathematical and Theoretical* **48**, 235301 (2015).